J. Fluid Mech. (1973), *vol.* 61, *part* 2, *pp.* 337–365
Printed in Great Britain

An experimental study of nonlinear disturbance behaviour in natural convection

By YOGESH JALURIA AND BENJAMIN GEBHART
Sibley School of Mechanical and Aerospace Engineering, Cornell University, Ithaca, N.Y.

(Received 26 December 1972)

An experimental investigation has been carried out to determine the behaviour of three-dimensional disturbances in laminar natural convection flow adjacent to a flat vertical surface with uniform heat flux input. A controlled two-dimensional disturbance, with a superimposed transverse variation, was introduced into the boundary region by a vibrating ribbon. The downstream propagation and amplification of these disturbances were studied in detail. Of principal interest was their nonlinear interaction with the base flow and any secondary mean flows that might arise therefrom. Measurements of the transverse mean velocity component indicate a double longitudinal vortex system. These results also show a distortion of the longitudinal base velocity profile which rapidly increases downstream. An alternate spanwise steepening and flattening of the profile is found to result. These mean flow modifications are found to be in good general agreement with existing theoretical and experimental studies of such flows. Our results are also compared with those obtained for forced flow. Several very important differences and similarities are indicated.

1. Introduction

One of the most important questions to be answered about any natural convection flow is whether the flow is laminar or turbulent, since the transport processes are strongly dependent on the flow regime. An understanding of the basic processes underlying transition from laminar to turbulent flow has, therefore, been the object of interest of many investigators in the past few years of rapidly increasing interest in the buoyancy-induced flows which predominate in the natural world around us.

In considering the question as to how and when laminar natural convection flows become turbulent, a study of laminar instability and of its subsequent importance in transition to turbulence is of great significance. Such studies deal with the behaviour of disturbances introduced in the flow through natural or artificial means and concern the conditions which enhance or curb amplification. Principal interest is in disturbances that amplify as they are convected downstream and on the interaction of such disturbances with the base flow. The important matters are how and why disturbances grow and by what mechanism they lead the flow to break down and to subsequent transition to turbulence.

It is generally not feasible in experiments to depend on disturbances which

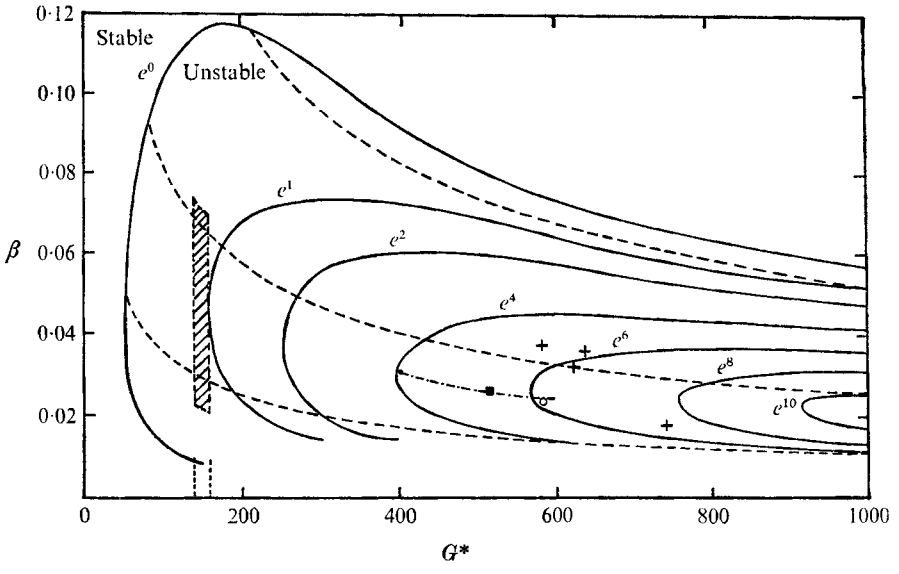

FIGURE 1. Stability plane for Pr = 6·7 (Hieber & Gebhart 1971) showing amplitude ratio contours in the unstable region. Cross-hatched area denotes ribbon location, in G^*, and range of frequencies used, in β. $q'' = 63{\cdot}2$ B.Th.U./h ft^2. Frequencies of maximum amplification, from figure 4: ●, $G^* = 405$; ■, $G^* = 530$; ○, $G^* = 575$. –·–·–, $\beta G^{*\frac{1}{2}} =$ constant = 0·60 curve for $f = 0{\cdot}08$ Hz. Natural disturbances: +, from Knowles & Gebhart (1969).

enter the boundary region from random sources, i.e. 'naturally' occurring disturbances. The most significant results have been obtained from studies of disturbances artificially introduced into the boundary layer. Since natural disturbances consist of many frequencies, it is not reasonable to attempt to simulate their magnitude and nature. Therefore, the phenomenon of boundary-layer instability and the effects of disturbance parameters like frequency, amplitude, etc., on the growth pattern are studied in a controlled experiment in which all such quantities may be systematically varied, according to the needs of the experiment.

Since it is believed that upstream disturbances cause later breakdown, it is reasonable to seek first a thorough understanding of the initial stages of the total process of transition. The initial growth or decay of small disturbances which enter a laminar flow has been treated analytically through linear stability theory. Such theory was applied initially to forced flows. The first similar consideration of laminar instability in natural convection was the establishment of the stability equations by Plapp (1957). Nachtsheim (1963) gave the first numerical solutions of the coupled disturbance equations. Recent years have seen much additional analytical and experimental investigation of this mode of instability, see Gebhart (1973). For natural convection over a flat vertical surface, the predictions of linear theory have received support from the experimental findings of Colak-Antic (1964), Polymeropoulos & Gebhart (1967), Dring & Gebhart (1969*a*) and Knowles & Gebhart (1969). The studies of Pera & Gebhart (1973) and of

Mollendorf & Gebhart (1973) for other flow configurations also show less complete, but good, agreement between the results of linear stability theory and experiment. It may now be inferred from these results that linear stability theory has given very satisfactory and valuable predictions of both the initial instability and the early growth of disturbances.

Linear stability analysis initially indicates the response of the flow to a two-dimensional disturbance. The resulting stability plane is in terms of a non-dimensional disturbance frequency β and a local Grashof number, see figure 1. For a uniform heat flux surface the Grashof number G^* is defined as

$$G^* = 5(g\beta_T q'' x^4/5k\nu^2)^{\frac{1}{5}},$$

where x is the distance along the vertical surface from the leading edge, q'' the uniform surface flux, k the thermal conductivity, ν the kinematic viscosity, β_T the coefficient of thermal expansion and g the acceleration due to gravity. The neutral curve e^0 indicates the frequency and Grashof number conditions beyond which disturbances begin to amplify. On one side there is a stable region and on the other side an unstable one. The significance of this plane is that, if we pick particular values of G^* and β, we have an indication of whether or not the disturbance will amplify locally.

A very striking result has been obtained from these calculations of disturbance amplification rates in flows adjacent to vertical surfaces. A very narrow band of frequencies has been found to be subject to very rapid downstream amplification, see Gebhart (1973). This characteristic is seen on figure 1. Paths of the convection of a disturbance of any particular physical frequency $\bar{\beta}$ downstream are given by $\beta G^{*\frac{1}{2}} =$ constant, in these generalized co-ordinates. The dashed curves shown are for several values of $\bar{\beta}$. The solid curves in the unstable region indicate the values of G^* at which a disturbance of unit magnitude at neutral conditions has been amplified to a magnitude e^1, e^2, etc. The extreme narrowness of the highly amplified region at large G^* indicates very sharp filtering. Experimental observations of Eckert & Soehngen (1951), Polymeropoulos & Gebhart (1967), Knowles & Gebhart (1969), Szewczyk (1962) and Godaux & Gebhart (1973), for flows subject to natural disturbances, corroborate this prediction of filtering. Highly amplified disturbances were found at high Grashof numbers and their predominant frequencies fell in the narrow band of high amplification predicted by the analysis. This suggests, as does the analysis, that in any given flow a disturbance of almost a single frequency is selectively amplified downstream. We would expect that such highly amplified disturbances may eventually cause turbulent bursts of large amplitude, which would in turn lead to complete turbulence. In forced flow, bursts are thought to follow from highly amplified disturbances.

The important disturbances at the initial stages are taken to be two-dimensional, see Knowles & Gebhart (1968). Therefore, the first stability analysis treated disturbances of this form. We would expect these results to apply strictly only for disturbances of small amplitude. As the disturbances grow downstream transverse effects may also appear and be amplified. Nonlinear mechanisms will eventually become important and possibly in several ways. Thus, for highly amplified disturbances, typically in regions far downstream from

the neutral curve, two-dimensional linear theory will fail and three-dimensional, or transverse, and nonlinear effects must be included in a realistic analysis.

In most of the experiments, usually qualitative, dealing with eventual transition in natural convection flows, three-dimensional effects have been observed. Eckert, Hartnett & Irvine (1960) employed smoke threads for flow visualization in natural convection flow over a flat vertical surface in air. Two-dimensional waves appeared first, with wave fronts essentially normal to the flow direction. These amplified as they moved downstream. Then vortices arose normal to the flow direction and parallel to the flat surface, i.e. transverse vortices. Vortices with axes parallel to the flow direction were also observed. These latter longitudinal vortices indicate the presence of transverse effects in the process. Therefore, it is inferred that the disturbances were initially predominantly two-dimensional and that, at some stage, transverse effects became significant.

Colak-Antic (1964) used hot-wire anemometers to study the behaviour of controlled disturbances along a flat vertical surface in air. Although a transverse component of velocity was detected, no definite conclusions were reached regarding transition. In another study on a flat vertical surface in water (Colak-Antic 1962), longitudinal vortices were seen with the help of a special visualization technique. A double longitudinal vortex system was found; one vortex was close to the wall and the other extended far out into the boundary region.

In addition to these observations, the very fact that turbulent flow is a three-dimensional phenomenon indicates that at some point during transition some such three-dimensional effect must become significant. The analysis of Benney (1961; see also Benney & Lin 1960), as well as the subsequent experiments of Klebanoff, Tidstrom & Sargent (1961), both for forced flow, also led to the conclusion that three-dimensional effects are an essential part of transition of that flow. We may also reasonably expect that three-dimensional secondary mean flows are an important and necessary feature in natural convection transition.

The present work was undertaken to study the growth and propagation of three-dimensional disturbances in a natural convection flow. We have studied the detailed nature of three-dimensional disturbances, their growth and their subsequent interaction with the base flow. For such a mechanism it is very important to investigate any longitudinal rolls which may arise and the distance they extend across the boundary region. Another aspect of importance is the way in which vortices might modify the mean flow. For example a 'shear layer', a region of intense shear, might arise and may be expected to contribute to rapid disturbance growth. The later formation of concentrated turbulent bursts might be associated with such features.

The detailed experimental study of Klebanoff *et al.* (1961), in forced flow and with controlled three-dimensional disturbances, clearly indicated that longitudinal vortices arise through nonlinear three-dimensional phenomena. These measurements detected a spanwise distribution of single longitudinal vortices, stretching out into the boundary region from the wall. The development and growth of these disturbances downstream were also studied.

Audunson & Gebhart (1973) have analysed the interaction of two- and three-dimensional disturbances and have calculated the resulting nonlinear effects, in

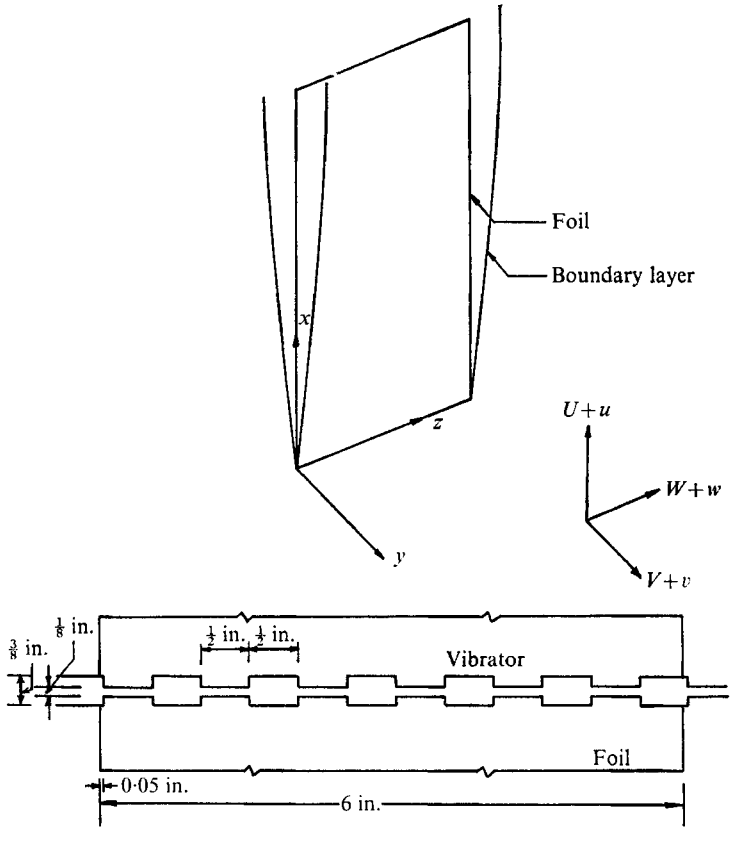

FIGURE 2. Definition of the co-ordinate system and the geometry of the vibrating ribbon.

a natural convection flow over a uniform flux, vertical surface in air. The sharp filtering found in these flows suggested an analysis similar to that of Benney (1961). These new calculations also indicate the presence of a system of mean-flow longitudinal vortices. It consists of an inner roll close to the wall and an outer roll stretching across the boundary region and out into the ambient fluid. These transversely alternating vortex pairs were inferred to give rise to an alternate spanwise flattening and steepening of the mean longitudinal velocity profile. This distortion of the base flow was found to increase downstream, for a particular disturbance frequency to which the flow is very unstable. Thus, regions of high and low shear, that is, local shear layers, are predicted. These could contribute to the mechanism of the eventual deterioration of the flow to turbulence.

In the present experimental study controlled two-dimensional disturbances, with a superimposed transverse variation, were introduced into the boundary-layer flow arising adjacent to a uniform surface flux, vertical surface in water. Their subsequent behaviour downstream was studied. The transverse variation was superimposed over a two-dimensional disturbance through a vibrating ribbon which had a spanwise variation in width, see figure 2. Disturbance propagation and growth were investigated with hot-wire anemometers.

A study of the consequences of naturally arising three-dimensional disturbances would be even more difficult than for natural two-dimensional disturbances, owing to the added spanwise co-ordinate. Continuous measurements would have to be taken simultaneously at many points along and across the vertical surface. This was not attempted in this study.

The measurements definitely established the presence of a double longitudinal vortex system in the boundary region. These vortices were inferred from measured variations, across the boundary layer, of a transverse mean velocity component which arose from nonlinear disturbance interactions. This component was found to change sign twice, suggesting a double vortex system. The presence of vortices was confirmed by measured transverse variations of this velocity distribution.

The inner roll lies very close to the wall. The outer one stretches far out in the boundary layer and even into the ambient medium, in accordance with the predictions of the analysis of Audunson & Gebhart (1973). The spanwise periodicity of the vortex system was determined from the measurements of the spanwise variation of the transverse mean velocity component. Measurements of the longitudinal mean flow velocity also indicated an alternate steepening and flattening of the profile around its inflexion point. Both the double vortex system and the points of high and low shear were found to have a spanwise periodicity identical to that of the transverse disturbance variation introduced into the boundary layer by the upstream vibrating ribbon.

In addition, the downstream growth pattern of the disturbances was measured at various spanwise locations. The frequency response of the flow was determined and the variation of the amplitude of such disturbances across the boundary layer was measured. It was found that the amplitude of the periodic part of the longitudinal velocity component varies in the spanwise direction. The measured spanwise locations of maxima and minima of its amplitude correspond closely to the maxima and minima of the disturbance introduced upstream by the ribbon.

2. The experiment

The experiment was carried out in water in a boundary layer generated adjacent to a uniform flux, flat, vertical surface. Water was chosen since high Grashof numbers are obtainable with a surface of reasonable height, even at temperature differences of the order of a few degrees, less than 5 °F in this study. Hollasch & Gebhart (1972; see also Hollasch 1970) have shown that, with water of high purity, at a resistivity around 1 MΩ cm, it is practical to make detailed velocity measurements with bare hot wires. Therefore, it was decided to use hot wires in pure water.

The flat surface which generated the flow was a stretched stainless-steel foil 0·001 in. thick and 6 in. wide. The foil was stretched vertically between two knife edges and was 27 in. high. It was adjusted to be vertical by a plumb bob and was heated electrically by means of a regulated d.c. power supply. The voltage across the foil was measured by a digital voltmeter and current through it by a shunt

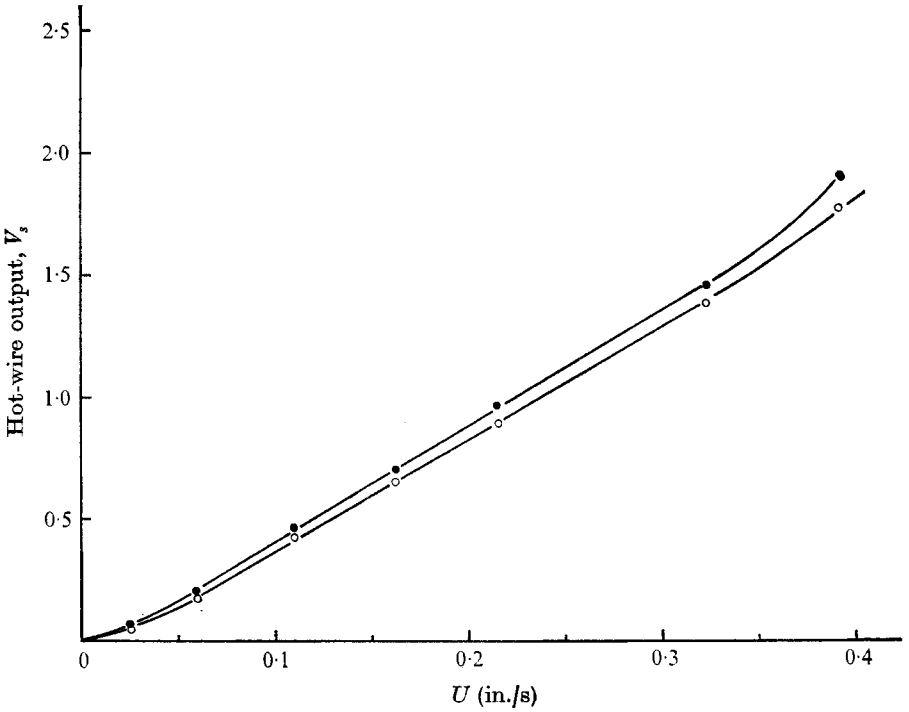

FIGURE 3. Hot-wire calibration curves. ●, resistance = 1·17 Ω; ○, resistance = 1.29 Ω.

resistance in series. The uniform foil thickness, manufacturing tolerance around 5 %, provided a uniform flux surface condition, since the flux is obtained from electrical dissipation.

The investigation was carried out in a 27 × 27 × 36 in. high tank made of glass walls supported by stainless-steel angles. Only stainless steel and teflon were used in the entire arrangement of foil, probes, vibrator, etc., as these were found by Hollasch & Gebhart (1972) to be non-contaminative to water.

Constant-temperature hot-wire anemometers (Disa model 55D01) were employed to measure both fluctuating and mean velocity components. Measurement of longitudinal velocity required only one hot wire. Two wires in a V-arrangement were used to measure the transverse component. The hot-wire supports were silver plated and the sensor wire was 0·0005 in. diameter platinum. The silver supports provide 'anodic protection' for the platinum wire as mentioned by Hollasch & Gebhart (1972). This reduces the drift in the calibration of the hot wire.

The hot-wire probes could be positioned at any point in the boundary region. Vertical and transverse locations were measured by scales with divisions of 0·05 in. and the position normal to the foil (in y) was determined by a micrometer with divisions of 0·001 in. The position of the surface was determined by an electrical circuit as described by Jaluria (1972).

Calibration of the hot wires was carried out by the technique developed by Dring & Gebhart (1969*b*). Water having a resistivity of about 1 MΩ cm was

used and the probe was held stationary in fluid translating vertically upwards. The relation between the velocity and buoyancy effect during calibration was the same as it was later during the measurements of the longitudinal component of velocity. In the transverse velocity component measurements, the relation was different. However, the effect is expected to be negligible, since the transverse velocity component is a very small perturbation to the longitudinal component.

The velocity range during calibration was 0–0·4 in./s, the range expected in this investigation. Calibration curves for two hot wires, of resistance 1·17 and 1·29 Ω, are shown in figure 3. All the hot wires employed in the study had a resistance of 1·17 Ω. The second curve is shown only to indicate the influence of the hot-wire resistance on calibration. Both the curves are seen to be linear over the velocity range 0·03–0·33 in./s and are concave upwards outside this range.

The hot-wire signals were recorded on a two-channel Offner dynograph (type RS). The overheat ratio of the hot wires was always 1·1. The sensor temperature at this overheat ratio is about 60 °F above the surrounding temperature. Since the temperature excess of the hot wire is much greater than the temperature variation across the boundary layer, the error in the calibration curve due to background temperature changes across the boundary region is negligible.

The controlled disturbance was introduced into the boundary layer by a ribbon parallel to the z axis and vibrating normal to the foil. The ribbon (0·001 in. thick and 7 in. wide) had a transverse variation in height, as seen in figure 2, to superimpose a transverse variation on the two-dimensional disturbance. The motion of the ribbon was sinusoidal and its amplitude and frequency could be controlled and measured. The arrangement employed was similar to that of Knowles & Gebhart (1969), except for the transverse variation in ribbon height. The ribbon could be positioned anywhere in the boundary region, in x and y.

The positioning of the vibrating ribbon is an important matter. First, the disturbance must be introduced into a flow region which is unstable or soon to be unstable to two-dimensional disturbances. However, since neutral conditions for transverse effects are not known, it is not possible to know if the chosen vibrator location is actually in a flow which is unstable to these effects.

The ribbon was placed at $x = 4$ in., which spans a range of G^* of 140–160 for the power input levels used in this study. This is downstream of the known neutral curve. A ribbon frequency of 0·08 Hz was chosen for most of the detailed measurements and for reasons set forth later. This frequency path, for the frequency and a typical value of the surface heat flux used in the experiments, is drawn in figure 1 over the downstream range of G^* studied (400–600). The ribbon location in terms of G^* and β, for all measurements made, is also shown as the cross-hatched region on figure 1.

The ribbon was positioned just outside the inflexion point of the base velocity profile. The advantage of this location is that the slope of the profile is more or less uniform in this region. Therefore, if the mean position (in y) of the vibrator is shifted somewhat, there should be no large change in the velocity disturbance imparted by a given ribbon vibration amplitude. Ribbon amplitudes were usually less than 0·003 in., compared with a velocity boundary-layer thickness of about 0·7 in. The disturbances were introduced at low enough values of G^* (140–160)

to allow the boundary layer to interact with the input disturbance over a sufficiently long time and distance before measurements were taken downstream.

Steady flow was attained within a few minutes, owing to the low thermal capacity of the foil. Initial measurements showed that test times up to 25 min could be employed without appreciable stratification or circulation arising in the tank. All measurements were made at z locations at least 1 in. from the edge of the heated surface, to avoid end effects.

It is to be noted that the downstream value of G^* at which nonlinear effects will become important depends on the magnitude of the input disturbance. Small input disturbances give the flow some distance in which to adjust the disturbance to a form consistent with disturbance growth mechanisms well before the amplitude is large enough to result in significant nonlinear effects. Thus, with initially small disturbances, it might be possible to study some aspects of the three-dimensional nature of the disturbances as they are convected downstream in the absence of significant nonlinear effects.

3. Experimental results

The disturbance introduced into the boundary layer by the ribbon is two-dimensional with a superimposed transverse variation. The resulting velocity disturbances and mean flow were measured downstream in the G^* range 400–600, indicated in figure 1. For the ribbon, figure 2, the middles of the portions of greater ribbon height are termed maxima and those of the portions of smaller height minima. These transverse positions are of special importance in this study.

The local mean flow is the sum of the base flow and of any secondary mean flow which has arisen through interaction among the disturbances or because of their interaction with the base flow. The three mean flow components are denoted by U, V and W and the base flow by U_b and V_b. Note that $W_b = 0$. Thus $U - U_b$, $V - V_b$ and W are the components of the secondary mean flow. The periodic parts of the velocity components are denoted by u, v and w. The quantities measured were the longitudinal and transverse components of the mean flow (U and W) and the amplitudes and frequencies of u and w. Their distributions were determined across the boundary region (in y) at various transverse positions z and at various downstream locations x.

Effect of disturbance frequency

The first important question is whether or not the transverse variation superimposed on the two-dimensional disturbance affects the 'frequency filtering' mechanism found to be characteristic of these base flows, see Gebhart (1973). In our first experiments the frequency of the vibrator was varied, at constant disturbance amplitude. Measurements were made at different downstream locations x and at z corresponding to both a maximum and a minimum. The hot wire was located between the peak and the inflexion point of the base flow velocity profile. The local maximum of the amplitude of the longitudinal component of the velocity disturbance u had been found both from theory and experiment to be at this location in the boundary region, see Gebhart (1969).

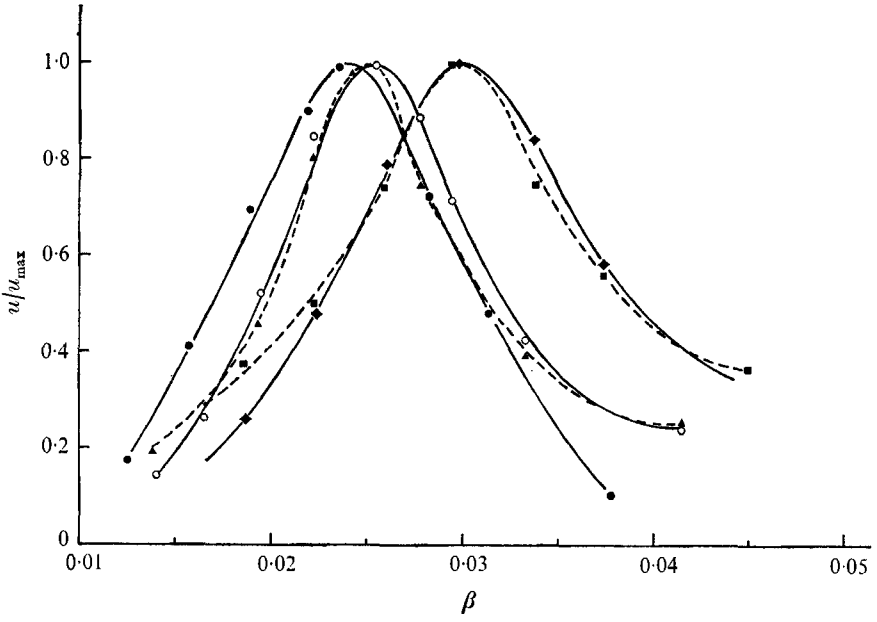

FIGURE 4. Variation of the amplitude of the longitudinal component of the velocity disturbance u with the frequency of the input disturbance at a maximum (solid curves) and a minimum (broken curves). At a maximum: ◆, $G^* = 405$; ○, $G^* = 530$; ●, $G^* = 575$. At a minimum: ■, $G^* = 405$; ▲, $G^* = 530$.

Our subsequent investigation of the variation of the amplitude of u across the boundary region again confirmed this.

The hot wire was placed parallel to the foil and horizontal, i.e. parallel to the z axis. This orientation measures the longitudinal component U of the mean velocity and the periodic component u. In the range of the Grashof number and input disturbance amplitude investigated, the measured u was sinusoidal.

The amplitude of u is plotted against the frequency of the input disturbance. The results are best considered in terms of the characteristic length δ and velocity U^*:

$$\delta = 5x/G^*, \quad U^* = \nu G^{*2}/5x, \quad \eta = y/\delta = yG^*/5x,$$

where η is the similarity variable and G^* is the local Grashof number, for a uniform flux surface. The disturbance frequency f ($\bar{\beta} = 2\pi f$) and wavenumber $\bar{\alpha}_R = 2\pi/\lambda$ are non-dimensionalized as

$$\beta = (\delta/U^*)\,\bar{\beta} = (25\bar{\beta}x^2)/\nu G^{*3}, \quad \alpha_R = \delta\bar{\alpha}_R.$$

The response of the boundary layer to disturbances of constant amplitude but of varying frequency is seen in figure 4. The amplitude of the periodic component u is normalized by u_{max}, the maximum amplitude measured over the frequency range at that downstream location, i.e. at that value of G^*. This ratio is plotted against β. A pronounced frequency filtering effect is seen for both z locations. Each curve peaks near a particular value of β. For values of frequency outside the range shown, the signal was too small to be reliably detected against the background of noise.

It is apparent from these results that the boundary layer amplifies input frequencies selectively and only over a very narrow range of frequencies. This agrees with the predictions of the linear stability theory for two-dimensional disturbances, see Gebhart (1973). Another significant result is the shift of the value of β for maximum amplification towards smaller values as G^* increases. This again agrees with the linear stability theory results. In fact, it is found that these peaks occur, for both the transverse locations, at values of β almost exactly equal to those predicted by linear stability theory to be most highly amplified at the values of G^* where measurements were taken. See the points at these peaks plotted on figure 1.

We see from figure 4 that the amplitude curves at the two transverse locations corresponding to a maximum and a minimum are very similar. For each value of G^* the peaks are found at almost the same values of β. Both shift to lower values of β with increasing G^*. However, the peak regions at a minimum are somewhat narrower.

The value of β at the peak is seen to range from about 0·03 to 0·024 as G^* increases from 405 to 575. However, the corresponding physical frequency f was approximately constant, about 0·08 Hz. Thus, it is approximately a single frequency that is most highly amplified in the flow.

As indicated above, the path of the downstream convection of a disturbance of constant physical frequency in (β, G^*) co-ordinates is $\beta G^{*\frac{1}{2}} = \text{constant}$. The path drawn on figure 1 in the range $G^* = 400$–600 is for $f = 0{\cdot}08$ Hz. It was calculated for the heat flux level typical of our experiments, $q'' = 63{\cdot}2$ B.Th.U./h ft^2.

The above results indicate that a spanwise variation in the input disturbance does not significantly affect the frequency response of the boundary layer to two-dimensional disturbances. Therefore, a frequency of 0·08 Hz was chosen for the input disturbance in our subsequent investigations of other aspects of disturbance growth. In all measurements downstream, u was found to be sinusoidal at the frequency of the input disturbance.

Amplitude of u vs. η

When the frequency of the vibrator had been chosen, the variation of the amplitude of u with y, or η, i.e. across the boundary region, was studied. This characteristic is important for two reasons. First, amplification mechanisms for three-dimensional disturbances might be apparent in changed forms of this distribution at various transverse locations. In the absence of transverse effects the form of this distribution would not be expected to vary across the width of the foil. Second, in order to detect the true downstream amplification rates of disturbances, it is necessary first to know how u varies across the boundary region and where its amplitude is a maximum.

The variation of the amplitude of u across the boundary region was measured at a number of spanwise locations. Since our interest lies mainly in the form of this distribution, rather than in actual local values, the measured distributions were normalized by $u_{\max}$, the maximum value measured across the boundary region (in η) at that value of z and G^*. The distributions obtained at a transverse location corresponding to a maximum of the input disturbance are shown in

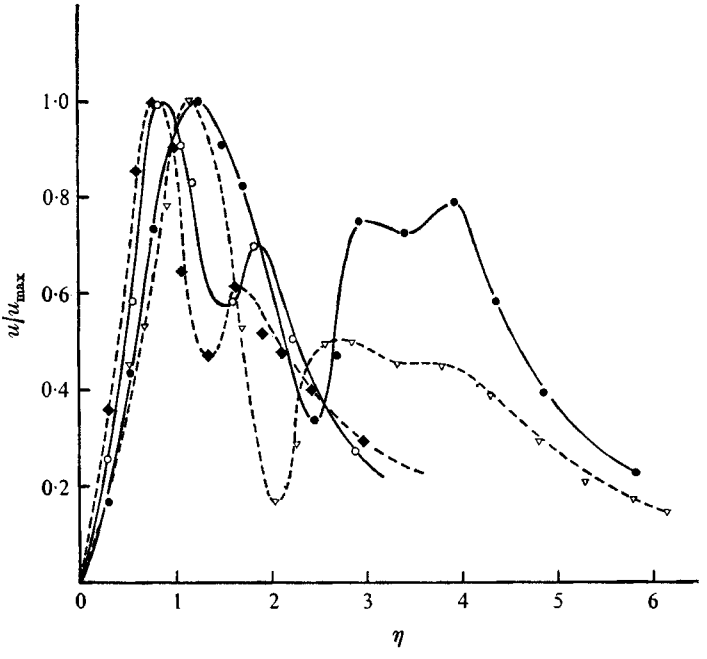

FIGURE 5. Distribution of the amplitude of u across the boundary region at a maximum. ◆, $G^* = 405$; ○, $G^* = 460$; ▽, $G^* = 530$; ●, $G^* = 575$.

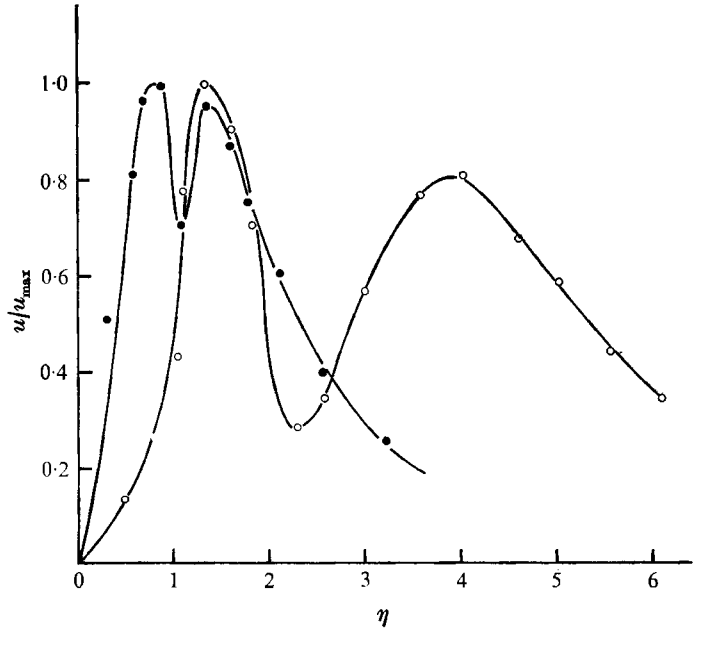

FIGURE 6. Distribution of the amplitude of u across the boundary region at a minimum. ●, $G^* = 460$; ○, $G^* = 530$.

figure 5, for $G^* = 405$, 460, 530 and 575. Those obtained at a minimum, and for $G^* = 460$ and 530 are seen in figure 6.

The form of these amplitude curves is seen to change with G^* and also with transverse position. All the curves have two peaks. The first one is very close to the surface, for all values of G^*, and is at around $\eta = 1{\cdot}0$. This agrees with the theoretical study of Knowles & Gebhart (1968). The second peak is much broader for higher G^*. As G^* increases, both the peaks shift toward higher η.

The change in these distributions with an increase in G^* is similar to the theoretical findings of Dring & Gebhart (1968) and to the measurements of Dring & Gebhart (1969*a*) in a light silicone oil, $Pr = 6{\cdot}7$. We found the outside peak to be lower in height than the inside one, being 50–80 % of its magnitude at a maximum and about 80–95 % at a minimum. No interesting conclusion has been drawn from such results concerning the effect of G^* on the relative height of the second peak.

These measurements have some interesting implications. If the disturbances at the two transverse locations had amplified independently of any transverse effect, then according to linear stability theory, the distributions at the two transverse locations would be very similar in form and differ only in the physical amplitude of u. However, these data show that they do not propagate independently. The transverse variation present in the input disturbance must cause these measured transverse modifications of the amplitude distributions.

It is conceivable that nonlinear interactions are solely responsible for this behaviour, instead of any purely periodic transverse amplification mechanism in the boundary layer. Any such nonlinear effect would be likely to become important less far downstream of the positions corresponding to maxima in the input disturbance than those corresponding to minima, since the amplitude of the initial disturbance is greater there. If nonlinear mechanisms do arise in the propagation of u, then its distribution at a maximum would deviate at lower G^* from the form of two-dimensional disturbances which applies in the linear range.

The above data were compared with the theoretical curves obtained by Dring & Gebhart (1968) and with the experimental results of Dring & Gebhart (1969*a*). The new data, at $G^* = 405$ and 460, match these curves more closely at a maximum than at a minimum. Therefore, it may be that the measured transverse variations in the form of u are, over this range of G^*, due to a periodic and linear transverse effect rather than to a nonlinear interaction. Recall that the input disturbances were very small. However, the forms of the curves at $G^* = 530$ and 575 are found to be very different, suggesting significant nonlinear effects.

The transverse variation of the amplitude of u

Since the x component U_b of the base flow velocity is much larger than the y component, it is expected that the u disturbance component is much greater than the v component. Therefore, u was considered characteristic of the disturbances and attention was focused on its transverse variation. The variation of u with z (at given y, or η) was measured to determine in more detail the nature of disturbance propagation downstream.

The measured amplitudes of u were normalized by the maximum value

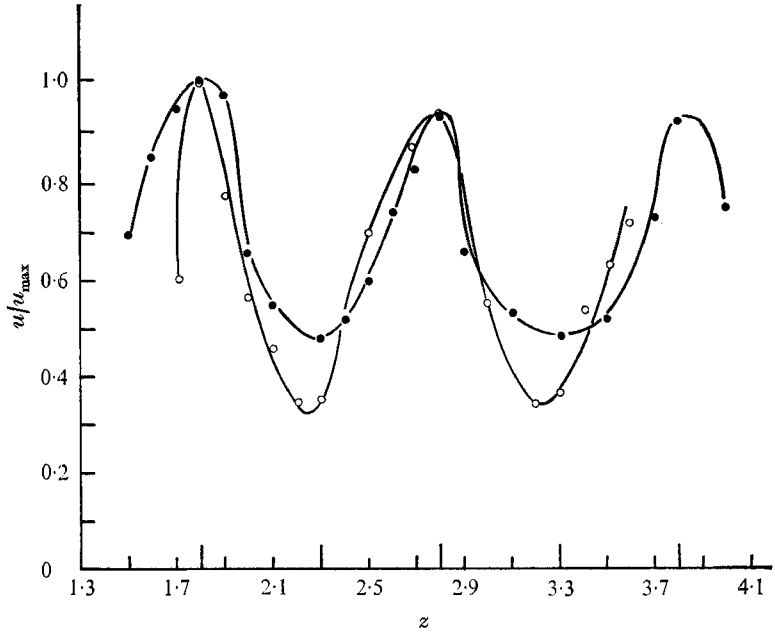

FIGURE 7. Spanwise distribution of the amplitude of u. ●, $G^* = 405$, $\eta = 0{\cdot}84$; ○, $G^* = 460$, $\eta = 0{\cdot}82$.

measured in the traverse across the surface, again called u_{max}. The results at $G^* = 405$ and 460 are shown in figure 7. The data were taken at $\eta = 0{\cdot}84$ for $G^* = 405$ and at $\eta = 0{\cdot}82$ for $G^* = 460$. Both these traverses were just outside the inside peak in the u distribution across the boundary region.

First, the peaks and valleys are very sharp. This is quite unlike the expected nature of the input disturbance, which is not expected to produce such sharp maxima or minima. Amplifying transverse effects are, therefore, accentuating the spanwise variation of u. A disturbance whose transverse effects are damped is expected to result in much flatter curves. These variations imply that these measurements were taken in the amplifying region for transverse effects. However, it is not possible to determine whether the disturbances had been initially introduced in the stable or unstable region for such transverse effects.

Another significant observation is the more or less vertical propagation of the disturbance pattern. The z locations of maxima and minima in the input disturbance, indicated in figure 7, continue to be the respective locations for peaks and valleys in the u *vs.* z distributions downstream. Klebanoff *et al.* (1961) found the same behaviour in forced flow. The initial spanwise positions of maxima and minima in u were preserved downstream.

However, we found that disturbances in the tank could lead to a z shift of the disturbance pattern. When such disturbances disappeared the pattern returned to its original position. This sensitivity to small disturbances is probably a consequence of the small velocities characteristic of natural convection flows. They are sensitive to very small effects.

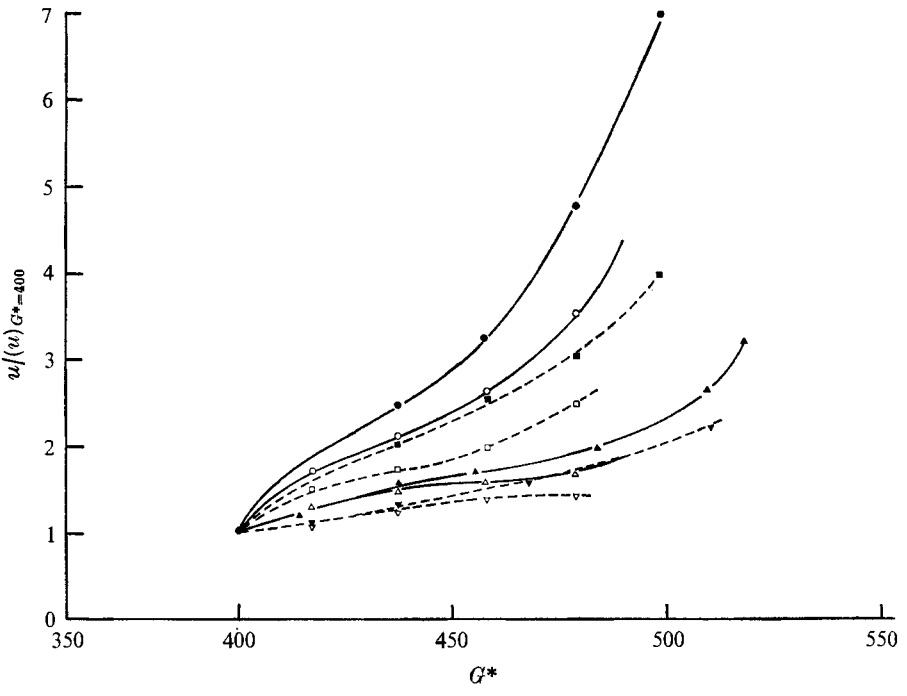

FIGURE 8. Downstream amplification of u, with G^*, for various amplitudes A of the input disturbance at a maximum (solid curves) and a minimum (broken curves). At a maximum: △, A = 0·002 in.; ▲, A = 0·003 in.; ○, A = 0·006 in.; ●, A = 0·007 in. At a minimum: ▽, A = 0·002 in.; ▼, A = 0·003 in.; □, A = 0·006 in.; ■, A = 0·007 in.

Disturbance growth downstream

The results thus far indicate that a strong transverse variation arises in the u component amplitude, even at a local G^* as low as 405. Even if the disturbance grew simply as a purely two-dimensional disturbance, we would still have a z variation, because of the form of the input disturbance. However, the sharp downstream peaks and valleys indicate amplifying transverse effects. Therefore, it was necessary to determine accurately whether these effects increase with G^*.

The rate of amplification, in terms of G^*, was measured for z locations corresponding to both a maximum and a minimum of the input disturbance. If the disturbance were to grow locally as a simple two-dimensional disturbance, the measured growth rates would be the same at the two transverse locations, within the range of linear amplification, even though the local amplitude in z would vary.

The disturbance growth rates were measured at various levels of input amplitude and at y = 0·17 in. This location corresponds to η = 0·91 and 0·86 for G^* = 400 and 500, respectively. The results are shown in figure 8. The ribbon amplitudes A were 0·002, 0·003, 0·006 and 0·007 in. The measured local amplitudes of u are normalized by its value at G^* = 400, the lower limit of the Grashof numbers investigated in this study. The region immediately downstream of the vibrating ribbon was avoided because the velocity disturbance is very small there, making accurate measurements difficult. Also, the physical form of the

disturbance would be expected to be quite artificial for some distance downstream of the ribbon.

The local G^* was varied by changing x for the curves corresponding to input amplitudes of 0·002, 0·006 and 0·007 in. For $A = 0{\cdot}003$ in. G^* was changed by varying the surface heat flux q''. The measured amplification rates appear to be independent of the way in which G^* is varied.

For very small input disturbance amplitudes, $A = 0{\cdot}002$ and 0·003 in., the growth rate at each transverse location is seen to be independent of A up to about $G^* = 440$. Linear processes clearly dominate in this range, even though the growth rate is significantly less at a minimum. A comparison of the measured amplification rates at a maximum with those predicted by linear stability theory supports this conclusion. The calculated ratio of the amplitude of u at $G^* = 450$ to that at $G^* = 400$, from figure 1, is 1·6. The measured value is 1·7. At a minimum it is 1·4. The same comparison over the G^* range 400–500 gives 3·0 *vs.* 2·3 at a maximum and 2·0 at a minimum. The small difference at a maximum may be due to a change in form of the u *vs.* η curves with G^*, rather than to significant transverse or nonlinear effects. Since the peak in the u distribution across the boundary layer shifts to higher η as G^* increases, the measured amplitude ratios would be expected to be lower than the calculated values for these measurements taken at a constant value of y. The larger difference at a minimum is perhaps due to other effects discussed later.

The measured amplitudes are also compared with the estimated magnitude of the velocity disturbance introduced at the ribbon. This magnitude is estimated as the difference between the velocities in the theoretical base velocity profile corresponding to the peak-to-peak positions (in y) of the vibrating ribbon. For $q'' = 63{\cdot}2$ B.Th.U./h ft^2, the velocity disturbance at the ribbon is calculated as 0·00106 in./s for $A = 0{\cdot}003$ in. The amplitude ratio contours on figure 1 also predict the velocity disturbance magnitude at $G^* = 400$ in terms of its magnitude at the ribbon, where $G^* = 140$. From these contours the amplitude of u at $G^* = 400$ is calculated to have been amplified to 0·0276 in./s. The experimentally measured velocity disturbance at $G^* = 400$ is 0·0033 in./s. This tenfold discrepancy suggests that this method of calculating the velocity disturbance induced by the ribbon is inaccurate. It would appear to be difficult to estimate the actual velocity disturbance introduced by the vibrating ribbon.

The curves on figure 8 for higher amplitude input disturbances, i.e. greater than 0·003 in., show significantly greater disturbance growth rates. This indicates significant nonlinear effects. The growth rate is seen to be a rapidly increasing function of the initial disturbance amplitude in this range of G^* and A.

As we have seen, the growth rate at the transverse location corresponding to a maximum in input disturbance is greater than that at a minimum. This difference in growth rates is found to be much greater at larger values of A. This is again due to nonlinear effects. However, even for small A, the difference in growth rates at the two positions is significant and we must conclude that these disturbance growth rates are affected by either linear or nonlinear transverse mechanisms, or by both.

We wished to determine whether the fact that the growth rate is greater at

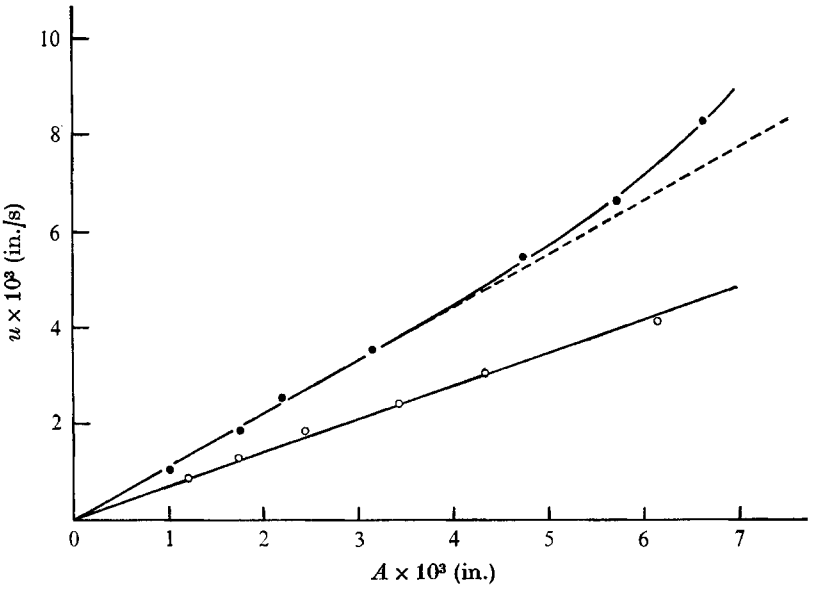

FIGURE 9. Variation of amplitude of u with the amplitude of the input disturbance A; $G^* = 405$, $y = 0{\cdot}16$ in. ($\eta = 0{\cdot}84$). ●, at a maximum; ○, at a minimum.

a maximum than at a minimum, even for low initial amplitudes and at G^* less than 440, is a linear consequence of the transverse disturbance effects or of a nonlinear interaction. Recall that, at higher values of G^*, nonlinear effects arise and cause the observed additional increase in the disturbance growth rate. The additional data of figure 9 suggest that the initial spanwise differences are due to linear transverse effects on u, at G^* around 400. The measured amplitude of u (at $G^* = 405$) is plotted as a function of the vibrator amplitude A at transverse locations corresponding to both a maximum and a minimum in input disturbance. The relation is clearly linear at small ribbon amplitudes, even though the amplitudes are different. Thus the growth mechanism of u is at least predominantly linear at all z.

At higher input amplitudes the growth rate increases at a maximum. In all our subsequent experiments the amplitude of the vibrating strip was limited to 0·003 in.

The transverse component of the velocity disturbance

These measured variations of the amplitude of u across the width of the foil imply at least a periodic transverse disturbance w. Since the input disturbance is periodic in time, as is u, we would expect w to be periodic at the same frequency. In addition, as the amplitude of u varies through the boundary layer (in y), we would expect that of w to vary also. In order to establish the very existence of a transverse disturbance component, and to verify these characteristics, measurements were made to detect w. However, we recall that the principal objective of this study is the nature of any secondary mean flow, in particular W, not the periodic component w of the transverse velocity. Therefore, only two experiments

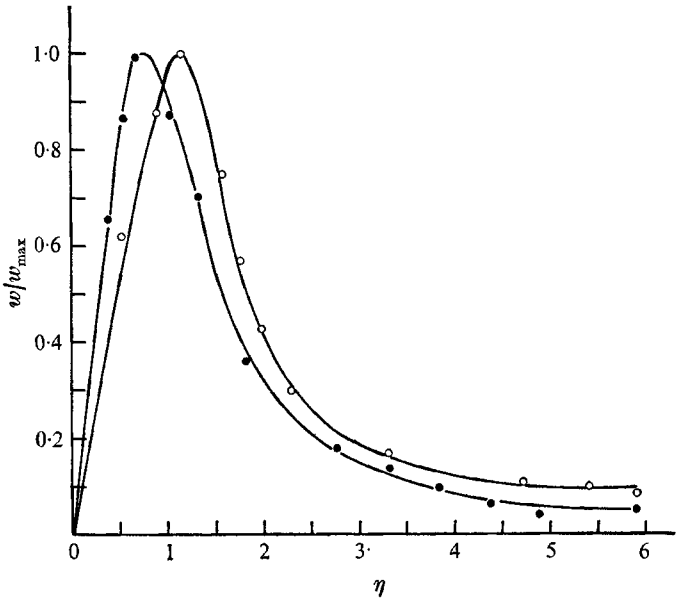

FIGURE 10. Distribution of the amplitude of the transverse component w of the velocity disturbance across the boundary region at $z = 3{\cdot}0$ in. ●, $G^* = 405$; ○, $G^* = 460$.

were carried out, at $G^* = 405$ and 460. These were both at a transverse location between a maximum and a minimum ($z = 3{\cdot}0$). A V-arrangement of two hot-wire probes, oriented in a plane parallel to the vertical surface, was used.

The measurements indicate that w is sinusoidal at the frequency of the input disturbance. The amplitude variation across the boundary region is plotted in figure 10. These curves are of w normalized by w_{max}, the maximum value measured in the traverse. The peaks in amplitude occur at around $\eta = 1{\cdot}0$, the region in which the amplitude of the u distribution also has a peak. The w disturbance extends all the way across the velocity boundary layer and, at its edge, is still 5–10% of its maximum value. The peak value shifts to higher values of η, and the distribution reaches out further into the boundary layer, at higher G^*, as does the u component amplitude distribution.

Secondary mean flow

Our primary interest was to detect and measure the nature of any secondary mean flow which might arise from a nonlinear interaction among spanwise-varying disturbances and/or the base flow velocity field. In particular we wanted to determine if any mean-flow longitudinal vortex system arises to distort the base flow.

Our earlier measurements on the growth of disturbances downstream indicated a predominance of linear growth mechanisms around $G^* = 400$, for A less than 0·003 in. Nonlinear effects were noticeable around $G^* = 440$. However, it must be noted that the growth rates were shown with the amplitude of the disturbance at $G^* = 400$ taken as unity. Therefore, it is to be expected that deviations from the linear processes would not be apparent immediately downstream.

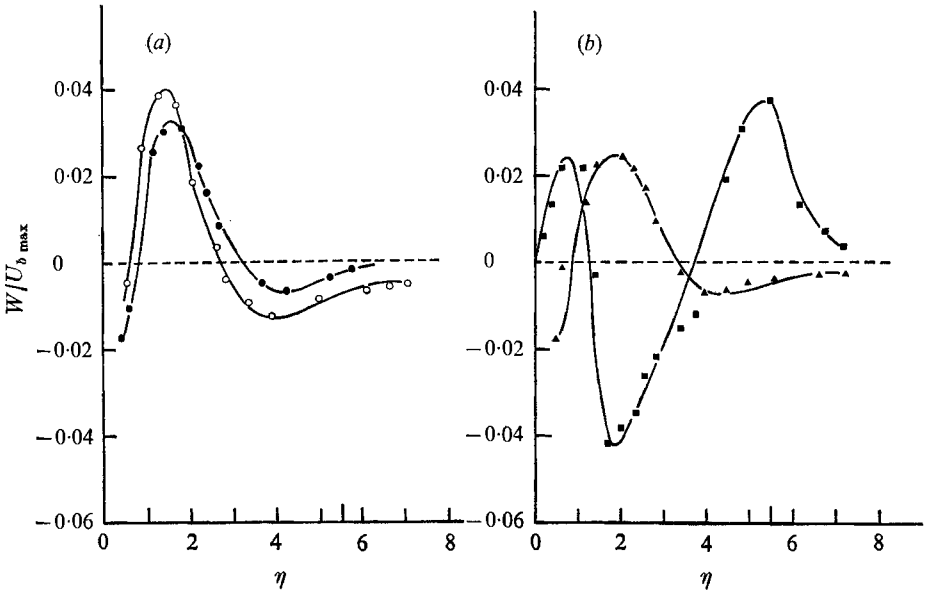

FIGURE 11. Distribution of the transverse component W of the mean velocity across the boundary region. (*a*) ●, $G^* = 400$ at $z = 3{\cdot}4$ in.; ○, $G^* = 460$ at $z = 3{\cdot}4$ in. (*b*) ▲, $G^* = 460$ at $z = 2{\cdot}75$ in.; ■, $G^* = 460$ at $z = 2{\cdot}90$ in.

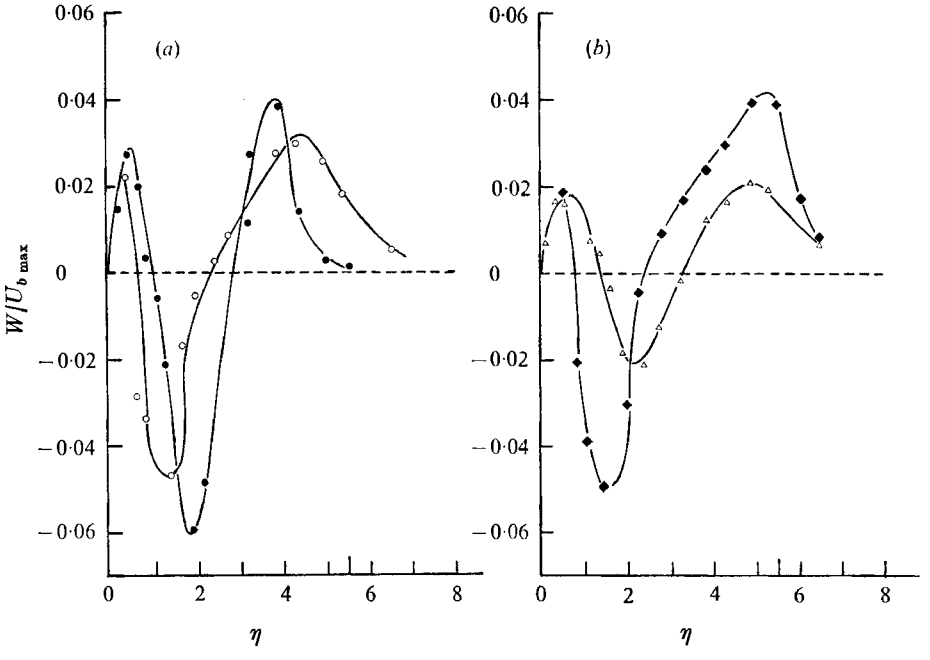

FIGURE 12. Distribution of the transverse component W of the mean velocity across the boundary region. (*a*) ●, $G^* = 460$ at 3·0 in.; ○, $G^* = 460$ at $z = 3{\cdot}1$ in. (*b*) △, $G^* = 500$ at $z = 2{\cdot}85$ in.; ◆, $G^* = 500$ at $z = 2{\cdot}95$ in.

Significant nonlinear effects give rise to Reynolds stresses which in turn cause a redistribution of momentum in the boundary region. This gives rise to the secondary mean flow. This could in turn modify the rate of energy transfer from the mean flow to the disturbances and subsequently their rate of growth. As indicated below, secondary mean flow was found to be present at $G^* = 400$, even though our measurements on u disturbance growth had not shown the presence of nonlinear effects until about $G^* = 440$.

To establish whether such a longitudinal vortex system is indeed a consequence of amplifying three-dimensional effects in the boundary layer, qualitative study may be undertaken by visualization techniques, e.g. those employed by Eckert *et al.* (1960) and by Colak-Antic (1962). Since considerable ambiguity is possible in such observations, we sought quantitative information concerning any such vortex system and undertook measurements of its location in and extent across the boundary region.

This required the accurate measurement, over the boundary region, of the transverse component W of the mean velocity. Taking W as positive along the positive z axis, changes in its sign across the boundary region (in y) would strongly suggest longitudinal vortex motion. A changing form of $W(y)$ with z might confirm it. For example, a single longitudinal roll vortex system would result in a $W(y)$ distribution which is once positive and once negative and with reversing characteristics in z. This behaviour was found by Klebanoff *et al.* (1961) in forced flow.

The same V-arrangement of hot-wire probes was again used. The difference between the mean signal of the two wires is the W component. Distributions of W *vs.* η were obtained by traversing the boundary region for the G^* range 400–500, at several transverse locations.

The results are shown in figures 11 and 12. In these curves W is normalized by $U_{b\,\max}$, the measured maximum velocity in the base profile without disturbances. The distributions in figures 11 and 12 (*a*) were measured at the transverse locations $z = 2{\cdot}75$, 2·9, 3·0, 3·1 and 3·4 in. for $G^* = 460$. Recall that one of the maxima in the input disturbance is at $z = 2{\cdot}8$ and the adjacent minimum is at $z = 3{\cdot}3$ in. These distributions show in detail the transverse variation of the W distribution. Figure 11 (*a*) also shows the distribution at $z = 3{\cdot}4$ in. for $G^* = 400$ and, therefore, indicates the changing form of $W(\eta)$ with G^*, at this transverse location. Figure 12 (*b*) shows the distribution at both $z = 2{\cdot}85$ and 2·95 in. for $G^* = 500$.

Two distinct forms of curves are obtained. One form, corresponding to the two curves of figure 11 (*a*) and the one of figure 11 (*b*) at $z = 2{\cdot}75$ in., shows negative values of W at low η, near the surface, rises to a peak at positive W, then returns to negative values and a minimum before gradually dying out at large η. The second form, seen in figure 11 (*b*) at $z = 2{\cdot}90$ in. and in figure 12, does just the opposite. It starts with positive values of W, etc. In all results the tails, at large η, sometimes extend, with large values of W, well beyond the outer edge of the boundary region, which is found at $\eta \approx 5{\cdot}5$ and indicated in figures 11 and 12.

Since W must be zero at the wall for each distribution, there must be a local extremum in W very close to the wall, either a maximum or a minimum, for all of these distributions. This extremum has been mapped in some later measure-

ments by going very close to the wall. Our earlier traverses were not carried very close to the wall because of fear of a 'wall effect'. However, in later measurements we found no significant effect of the heated surface on the hot-wire signal, even at very small distances from it.

In forced flow the comparable boundary layer is much thinner than in natural convection and the physical distance from the wall for similar values of η is much less. Thus readings may be distorted, as Klebanoff *et al.* (1961) concluded for their results. However, it is interesting to note that these investigators chose to ignore readings very close to the wall which might have, in fact, substantiated the presence of a second inside vortex. We think that our measurements very close to the wall, even at $\eta = 0{\cdot}2$, are reliable and accurate.

All the results indicate that W changes sign twice as the boundary region is traversed. This points to the presence of a double longitudinal vortex system. This is confirmed by the variation of the W distribution across the width of the foil, as we shall see.

First, the distributions of W shown in figure 11 (*a*) for both $G^* = 400$ and 460 at $z = 3{\cdot}4$ in. (a minimum is at $z = 3{\cdot}3$ in.) are seen to be similar. The peak value of W occurs around $\eta = 1{\cdot}7$. The two sign reversals suggest the centres of two rolls, since on one side of each centre the transverse velocity is in one direction and on the other in the opposite direction. Assuming two rolls, the location of their interface is logically taken as the highest absolute value of W between the locations of the two zero values. At this interface two vortices augment each other. The inner roll extends from $\eta = 0$ to approximately $\eta = 1{\cdot}7$. The outer roll occupies the region from 1·7 to 7, and even beyond. At the higher G^* the outer roll extends out further beyond the edge of the boundary region; the extent of the inner roll seems unchanged. These curves also indicate that the value of $W/U_{b\,\max}$ at the interface increases with G^*. This increase in three-dimensional effects with G^* is consistent with our earlier measurements.

The curves shown in figures 11 and 12 confirm the presence of a two-roll longitudinal vortex system. Figure 11 (*b*) shows a reversal in form from $z = 2{\cdot}9$ to $z = 2{\cdot}75$ in. Thus there is a plane of demarcation between these transverse locations. On opposite sides of this plane the vortices rotate in opposite directions. The input maximum, at $z = 2{\cdot}8$ in., is seen to be a plane of demarcation. Since the maxima and minima in the input disturbance are also locations of symmetry, zero mean transverse flow is expected at these locations. Similarly, the different forms of the curves in figure 11 (*a*) at $z = 3{\cdot}4$ and in figure 12 (*a*) at $z = 3{\cdot}1$ indicate the presence of another plane of symmetry for counter-rotating vortices and we would conclude that the minimum in the input disturbance ($z = 3{\cdot}3$ in.) is also the dividing plane for two counter-rotating vortices. Measurements were also made at $z = 2{\cdot}8$ and 3·3 in. However, W was found to vary with time and was too small to be reliably measured. Thus, each pair of longitudinal vortices stretches (in z) from a maximum to a minimum.

To verify further the existence of such a longitudinal vortex pattern, W was measured as a function of z at $G^* = 460$, and also at 475, at $y = 0{\cdot}25$ in. The corresponding values of η are 1·47 and 1·45 for these values of G^*. These locations should put the hot wire near the interface of the two vortices, i.e. at a local

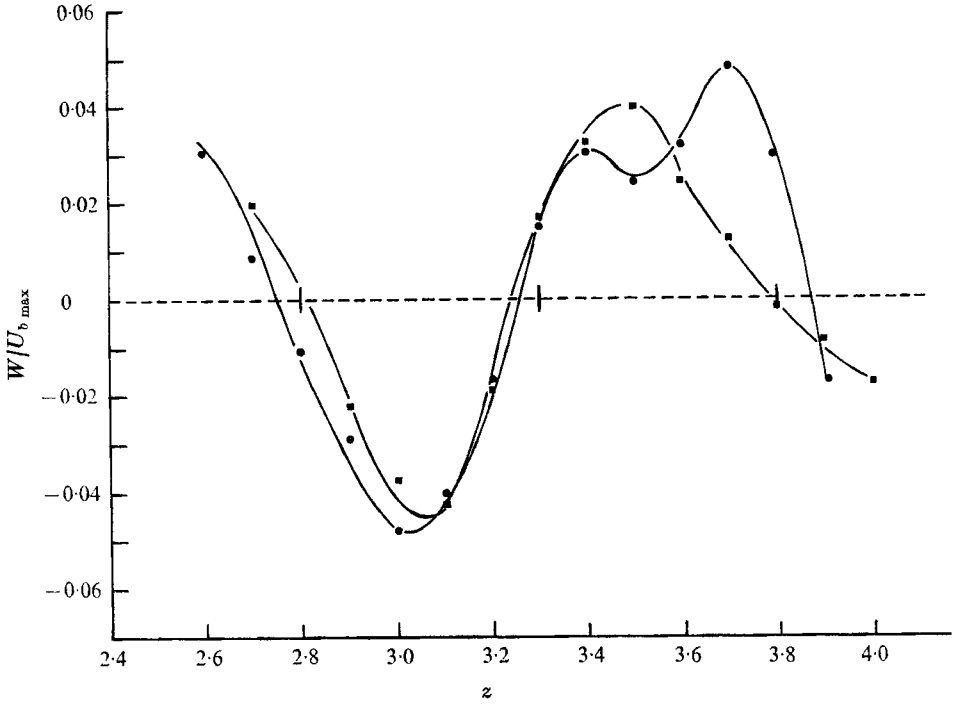

FIGURE 13. Distribution of $W/U_{b\,\max}$ in the transverse direction.
●, $G^* = 475$, $\eta = 1{\cdot}45$; ■, $G^* = 460$, $\eta = 1{\cdot}47$.

maximum in W. The results, in figure 13, indicate that one vortex pair extends from about $z = 2{\cdot}78$ to $z = 3{\cdot}26$ in. and that the adjacent one extends from $z = 3{\cdot}26$ to approximately $z = 3{\cdot}84$ in. This again shows that each vortex pair lies between a maximum and a minimum, located at $z = 3{\cdot}3$ and $z = 2{\cdot}8$ in. for the input disturbance. The slight difference may be due to a shift of the vortex pattern caused by the hot-wire sensors.

This collection of results also shows some other interesting things. The measured $W/U_{b\,\max}$ is seen to be always less than about 0·06. Thus the mean transverse velocity is very small compared with the longitudinal base flow component. However, we shall see in the next section that even this small transverse motion causes significant distortion of the longitudinal mean flow velocity profile U.

The location of the interface of the vortices is seen to be quite sharply defined, at $\eta \approx 1{\cdot}7$, unlike the locations of the centre and the outside peak in the outer vortex. Although the vortices are perhaps disturbed by the traversing of the hot-wire probes, particularly in the outer region of the outer vortex where the longitudinal velocity is small, these curves do confirm the transverse locations of the vortices. We also note that the peaks of the $W/U_{b\,\max}$ distributions (in y) are smaller in value near either a maximum or a minimum.

The picture of the longitudinal vortex system that emerges from these measurements is sketched in figure 14, on the basis of their average characteristics. Vortex pairs lie between adjacent maxima and minima. One vortex is close to the wall

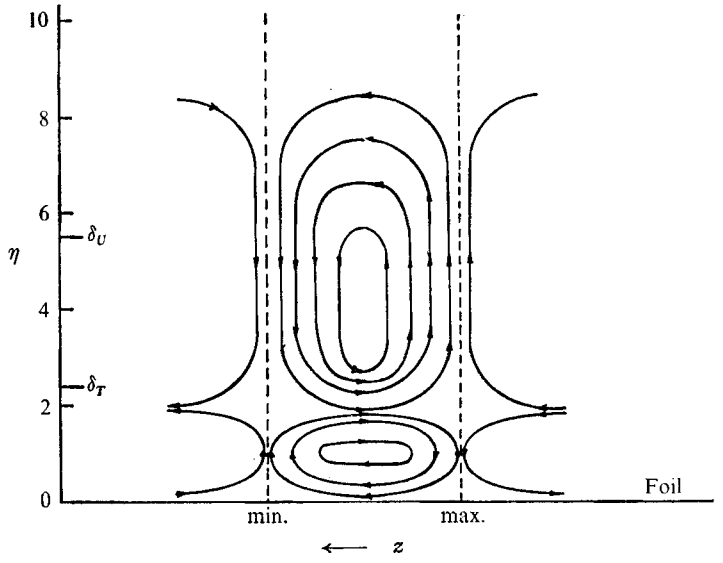

FIGURE 14. Sketch of the longitudinal vortex system, employing average values of η and W from figures 11–13.

and the other stretches out well beyond the boundary region. At a maximum in input, the outer vortex tends to convect fluid from inside the boundary region to the outside, whereas at a minimum it brings fluid into the boundary region from the quiescent medium. The importance of this mechanism is the resulting distortion of the base profile, as discussed in the next section. Here we only remark that these observations agree very well with the results of the analysis of Audunson & Gebhart (1973). Since those calculations were for air, no quantitative comparisons are attempted. However, a comparison of the present results with the calculated streamlines of the secondary mean motion indicates that, for water, the vortices are somewhat closer to the wall. These writers have pointed out that such a result is to be expected.

Distortion of the base velocity profile

We now consider the very important question of the distortion of the base velocity profile U_b by the secondary mean motion which the disturbances have generated in the boundary region. The mean longitudinal profile was measured in the absence of any disturbances and then again with the disturbances present. From the nature of the longitudinal vortex system we would expect the most significant modifications of this mean flow to occur at the maxima and minima of the input disturbance. The pumping action of the rolls in the y direction, where the largest gradients are found, should be strongest there. The transport effect of the vortices brings fluid into the boundary region from outside at the transverse position corresponding to a minimum in input. The reverse occurs at a maximum. Therefore, the longitudinal component U of the mean flow was measured at transverse locations corresponding to a maximum and a minimum.

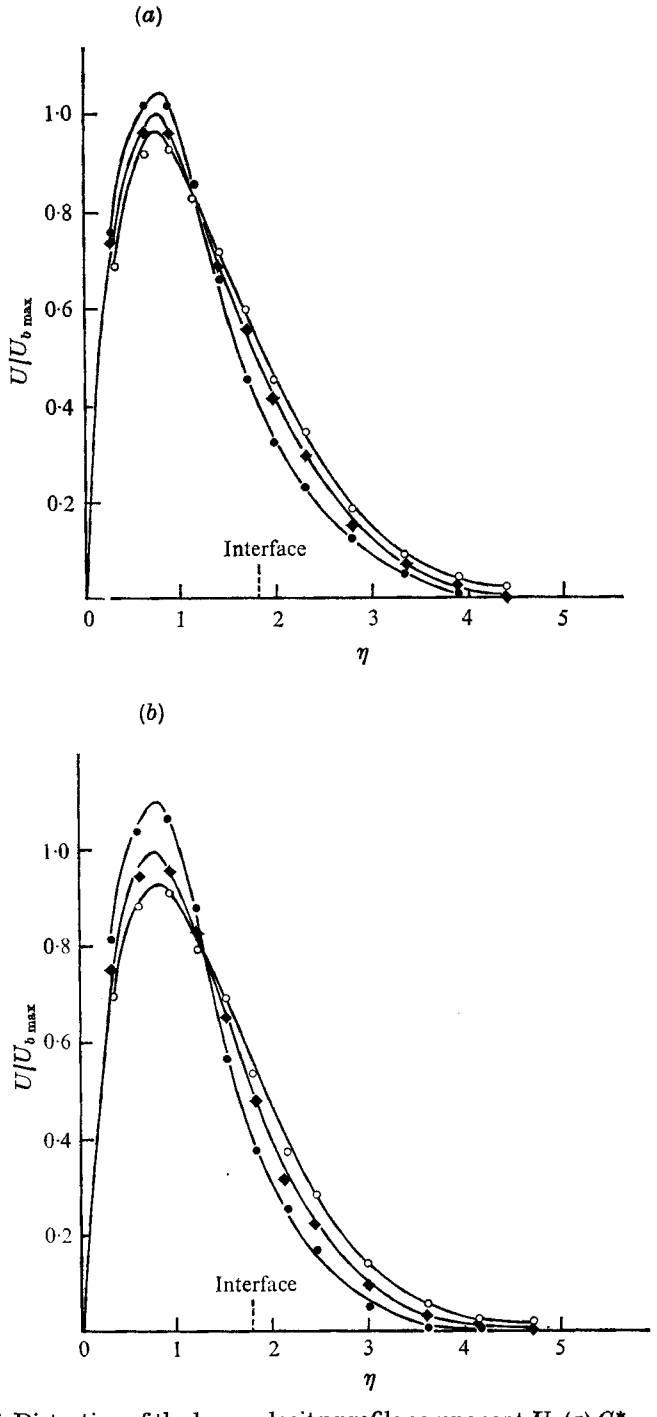

FIGURE 15. Distortion of the base velocity profile component U. (*a*) $G^* = 500$. (*b*) $G^* = 560$. ○, at a maximum; ●, at a minimum; ◆, measured base profile.

The base velocity profile was measured without disturbances at $G^* = 500$ and compared with the theoretical curve from Knowles (1967). The measured peak was found to be 7 % lower than the theoretical value. The disagreement near the edge of the velocity boundary layer was found to be higher. Therefore, the measured mean profile with the disturbances present was compared with the measured base profile, not with the calculated one. The results, in figures 15 (*a*) and (*b*) are the measured distribution U, normalized by the maximum value $U_{b\,\max}$ of the base flow velocity, plotted *vs.* η. Thus, the relative distortion due to the secondary mean flow generated by disturbances is seen directly.

At $G^* = 460$ any distortion was unmeasurable. Appreciable distortion was found at $G^* = 500$ and the amount at the peak of the base profile is seen in figure 15 (*a*) to be about 5 %. At $G^* = 560$ it is about 10 %, see figure 15 (*b*). At both values of G^* we see that the mean flow velocity maximum is greater than that of the base flow at the transverse position corresponding to a minimum in the input disturbance and less at a maximum.

The consequences of mean flow modification

The secondary mean flow has steepened the base flow profile around the inflexion point at a minimum. The profile is flattened at a maximum. Thus, there is an alternate steepening and flattening of the mean profile transversely across the surface. A region of steepening is called a 'shear layer' and these measurements indicate that this shear concentration becomes increasingly intense with increasing G^*. At such locations the disturbances are presumably fed by the mean flow at an increasing rate. This rapid growth may result in the bursts which we believe may also lead to turbulence in natural convection flows. The flattening of the base profile, on the other hand, causes a local thickening of the boundary region and may result in a concentration of buoyancy in small packets of fluid near the outside of the boundary region. That this mechanism may also lead to turbulence has also been suggested by schlieren observations in the present study. Therefore, at this stage of our knowledge, both steepening and flattening of the profile must be considered as possibly significant in the transition process.

These measured distortions of the mean flow profile are clearly the consequence of the longitudinal vortex system described earlier. At a minimum, the outer roll brings in cold stationary fluid from outside the boundary region, reducing the longitudinal velocity in the outer part of the boundary layer. On the other hand, the inner roll moves higher velocity fluid, from lower values of η, out towards this incoming fluid. The two processes together steepen the profile around the inflexion point. Although the inner roll also brings out fluid at lower velocity from closer to the wall, this fluid carries greater buoyancy with it, owing to the temperature gradient. This increases the velocity, as seen in the measured increase in the peak value of U in the profile.

At a transverse position corresponding to a maximum in the input disturbance, the outer vortex conveys higher velocity fluid towards the edge of the boundary region, thereby increasing the velocity there. The inner vortex moves lower velocity fluid from higher values of η to the region between the inflexion point and the peak of the base profile. The effect of this fluid of lower velocity, as well

as of lower buoyancy, is to reduce the peak value of the mean profile. As a result the profile is flattened around the inflexion point.

These interpretations suggest that, owing to the inner roll, the velocity peak would be shifted towards the outer edge of the boundary layer at a minimum and inwards at a maximum. However, the measured distributions do not show an appreciable effect.

In summary, it is found that the longitudinal velocity profile is increasingly distorted at higher values of G^* and that alternate regions of high and low shear, and of boundary region thinning and thickening, result.

4. Conclusions

These measurements indicate both the linear and nonlinear features of the growth and propagation of three-dimensional disturbances in a natural convection boundary layer. The results are in excellent agreement with the analysis of Audunson & Gebhart (1973) of nonlinear disturbance growth whose formulation is based on, and consistent with, the striking mechanisms of frequency filtering which characterize these flows. The evidence indicates that such three-dimensional effects are an essential part of boundary-layer instability mechanisms and that they may play an important role in the transition from laminar to turbulent flow.

Although these measurements were made in a flow subject to controlled disturbances, we believe that the mechanisms observed are also relevant to flows subject to natural disturbances. Random natural disturbances are the usual cause of transition in actual applications. These disturbances enter the boundary region from outside and would presumably consist of components of various magnitudes, frequencies and dimensionality.

It is already well established from much experimental observation that the flow responds selectively to such disturbances and rapidly amplifies the two-dimensional disturbance components and then in only a narrow band of frequencies. This two-dimensional effect dominates initially. Transverse variations do not quickly intervene. However, both calculations and the present measurements indicate that, further downstream, they begin to amplify and lead, through nonlinear interactions, to strong secondary mean flows.

Our measurements have conclusively shown that a double longitudinal vortex system arises from three-dimensional disturbance interaction. As the transverse variations of the disturbances grow, spanwise regions of higher and lower amplitudes of disturbances are accentuated. These transverse variations lead to the vortex system we have now mapped. This system induces a flow of quiescent fluid into the boundary region at some transverse positions and pumps fluid from inside to outside the boundary region at other positions.

This secondary mean flow distorts the longitudinal velocity profile. Near the inflexion point it is steepened at some locations and flattened at others. A steepened velocity profile is a region of intense shear, conventionally called a 'shear layer'. This intense local shear could cause the disturbances to grow at a much higher rate than at other spanwise locations. Given the sharp frequency

filtering which is abundantly substantiated in such natural convection flows, the secondary mean flows, as well as later events, are expected to be highly ordered. This characteristic has also been observed. Thus we now think it possible that this simple feature of the flow is the cause of breakdown. On the other hand, the flattened velocity profile causes a thickening of the boundary layer which may, as we have seen, also contribute to the deterioration of the flow to turbulence. However, detailed mechanisms beyond this initial distortion of the profile are now unknown.

For a uniform flux, vertical surface in a liquid, Knowles & Gebhart (1969), in silicone oil having a Prandtl number equal to that of water, found the first turbulent bursts at a G^* of 600–700. In cold water, at a Prandtl number of around 11·0, Lock & Trotter (1968) observed transition at $G^* = 430$–500. However, it is not clear that the criteria for the beginning of transition were the same. If from our data, with controlled disturbances, we take the beginning of transition to be the location where the base velocity profile suffers an appreciable distortion, the value is $G^* \approx 500$. This value is consistent with the appearance of bursts further downstream.

Further investigation of 'natural' transition will require a study similar to this one but which measures the consequences of naturally occurring disturbances. It would be necessary to know something of the initial three-dimensional nature of such disturbances and how their transverse characteristics grow downstream. The distortion of the base velocity profile would be measured and the downstream consequences of this distortion determined.

A comparison of our results with those obtained by Klebanoff *et al.* (1961) in forced flow shows some interesting differences. They inferred the presence of single longitudinal vortices in the boundary region, unlike our results, which indicate a double vortex system. Those vortices occupied only the inner half of the boundary region. On the other hand, our measurements show that the outer vortex stretches across the boundary region and out into the quiescent fluid. These vortices may, therefore, be expected to cause a greater distortion in the longitudinal mean velocity profile.

The change found in the peak value of the mean profile at maxima and minima of the disturbance amplitude is attributed to buoyancy effects and would, therefore, be found only in flows induced by a diffusion mechanism. Unlike our results, which show uniform steepening or flattening of the bas e velocity profile Klebanoff *et al.* (1961) found the development of an inflexion point at a maximum and a fuller profile than the Blasius at a minimum.

The authors wish to acknowledge support for this research under National Science Foundation Grant GK 18529 and support from the same grant for the first author as a research assistant.

REFERENCES

AUDUNSON, T. & GEBHART, B. 1973 Observations on the secondary three-dimensional mean motion induced by oscillations in a natural convection boundary layer. To be published.

BENNEY, D. J. 1961 A non-linear theory for oscillations in a parallel flow. *J. Fluid Mech.* **10**, 209.

BENNEY, D. J. & LIN, C. C. 1960 On the secondary motion induced by oscillations in a shear flow. *Phys. Fluids*, **3**, 656.

COLAK-ANTIC, P. 1962 Dreidimensionale Instabilitatser-Scheinungen des laminar-turbulenten Umschlages bei freier Konvektion langs einer vertikalen geheizhen Platte. *Sitz. Heid. Akad. der Wiss., Mathe.-natur Klasse*, p. 315.

COLAK-ANTIC, P. 1964 Hitzdraht messungen des laminar-turbulenten Umschlags bei freier Konvektion. *Jahrbuch W.G.L.R.*, p. 172.

DRING, R. P. & GEBHART, B. 1968 A theoretical investigation of disturbance amplification in external natural convection. *J. Fluid Mech.* **34**, 551.

DRING, R. P. & GEBHART, B. 1969*a* An experimental investigation of disturbance amplification in external natural convection flow. *J. Fluid Mech.* **36**, 447.

DRING, R. P. & GEBHART, B. 1969*b* Hot wire anemometer calibration for measurement at very low velocity. *J. Heat Transfer*, **91**, 241.

ECKERT, E. R. G., HARTNETT, J. P. & IRVINE, T. F. 1960 Flow visualization studies of transition to turbulence in free convection flow. *A.S.M.E. Paper*, no. 60-Wa-260.

ECKERT, E. R. G. & SOEHNGEN, E. 1951 Interferometric studies on the stability and transition to turbulence of a free convection boundary layer. *Proc. Gen. Disc. Heat Transfer, London*, p. 321.

GEBHART, B. 1969 Natural convection flow, instability, and transition. *J. Heat Transfer*, **91**, 293.

GEBHART, B. 1973 Instability, transition and turbulence in buoyancy induced flows. *Ann. Rev. Fluid Mech.* **5**, 213.

GODAUX, F. & GEBHART, B. 1973 An experimental study of the transition of natural convection flow adjacent to a vertical surface. *Int. J. Heat Mass Transfer*, to appear.

HIEBER, C. A. & GEBHART, B. 1971 Stability of vertical natural convection boundary layers: some numerical solutions. *J. Fluid Mech.* **48**, 625.

HOLLASCH, K. 1970 A survey of the literature, design, and experimental verification of a measurement scheme for external turbulent natural convection flow. M.S. thesis, Cornell University.

HOLLASCH, K. & GEBHART, B. 1972 Calibration of constant temperature hot wire anemometers at low velocities in water with variable fluid temperature. *J. Heat Transfer*, **94**, 17.

JALURIA, Y. 1972 The growth and propagation of three-dimensional disturbances in laminar natural convection flow adjacent to a flat vertical surface. M.S. thesis Cornell University.

KLEBANOFF, P. S., TIDSTROM, K. D. & SARGENT, L. M. 1961 The three-dimensional nature of boundary-layer instability. *J. Fluid Mech.* **12**, 1.

KNOWLES, C. P. 1967 A theoretical and experimental study of the stability of the laminar natural convection boundary layer over a vertical uniform flux plate. Ph.D. thesis, Cornell University.

KNOWLES, C. P. & GEBHART, B. 1968 The stability of the laminar natural convection boundary layer. *J. Fluid Mech.* **34**, 657.

KNOWLES, C. P. & GEBHART, B. 1969 An experimental investigation of the stability of laminar natural convection boundary layers. *Prog. Heat & Mass Transfer*, **2**, 99.

LOCK, G. S. H. & TROTTER, F. J. DE B. 1968 Observations on the structure of a turbulent free convection boundary layer. *Int. J. Heat Mass Transfer*, **11**, 1225.

MOLLENDORF, J. C. & GEBHART, B. 1973 An experimental and numerical study of the viscous stability of a round laminar vertical jet with and without thermal buoyancy for symmetric and asymmetric disturbances. *J. Fluid Mech.* **61**, 367.

NACHTSHEIM, P. E. 1963 Stability of free convection boundary layer flows. *N.A.S.A. Tech. Note*, no. D-2089.

PERA, L. & GEBHART, B. 1973 On the stability of natural convection boundary layer flow over horizontal and slightly inclined surfaces. *Int. J. Heat Mass Transfer*, **16**, 1147.

PLAPP, J. E. 1957 The analytic study of laminar boundary layer stability in free convection. *J. Aero. Sci.* **24**, 318.

POLYMEROPOULOS, C. E. & GEBHART, B. 1967 Incipient instability in free convection laminar boundary layers. *J. Fluid Mech.* **30**, 225.

SZEWCZYK, A. A. 1962 Stability and transition of the free convection boundary layer along a flat plate. *Int. J. Heat Mass Transfer*, **5**, 903.